Polymer-plasticizer compatibility during coating formulation: A multi-scale investigation

Ahmed Jarray, Vincent Gerbaud, Mehrdji Hemati

Polymer-plasticizer compatibility during coating formulation: A multi-scale investigation

A. Jarray[a,b,*], V. Gerbaud[a,b], M. Hemati[a,b]

[a] Université de Toulouse, INP, UPS, LGC (Laboratoire de Génie Chimique), 4 allée Emile Monso, F-31432 Toulouse Cedex 04, France
[b] LGC, INP, ENSIACET, 4 Allée Emile Monso, 31432 Toulouse, France

Keyword:
Plasticizer
Miscibility
Pharmaceutical products
Coating
Molecular dynamics

A B S T R A C T

During the formulation of solid dosage forms coating, plasticizers are added to the film forming polymer to improve the mechanical properties of the coating shell of the drug product. For the coating formulation to be successful and in order to produce flexible continuous film, the plasticizer should be compatible with the film forming polymer (i.e. high plasticizer-polymer miscibility in solid dispersion) (McGinity and Felton, 2008). This paper proposes and compares different multi-scale methods to predict the compatibility between plasticizers and film formers. The methods are based on, i) Molecule charge density using COSMO, ii) Solubility parameter calculation using Molecular dynamics, iii) Mesoscale simulation using DPD, where we propose a coarse-grain model, and iv) experimental DSC analysis for validation. The methods are tested for various blends including HPMC-PEG, MCC-PEG and PVP-PEG. The different methods showed similar results; PEG plasticizer diffuses inside HPMC and PVP polymer chains, thereby extending and softening the composite polymer. However, MCC surrounds PEG molecules without diffusing in its network, indicating low PEG-MCC compatibility. We also found that DPD simulations offer more details than the other methods on the miscibility between the compounds in aqueous solid dispersion, and can predict the amount of plasticizer that diffuse in the film forming polymer network.

1. Introduction

Polymeric film coatings are widely used for oral-controlled or sustained drug release. They generally consist of mixtures of various materials that are added to confer or enhance specific properties to the final product. Typically, a coating dispersion is composed of water, film-forming polymer, plasticizer and other additives such as fillers and stabilizers.

Today, important difficulties in polymeric coating formulation are; a) the assessment of polymer-plasticizer interaction, b) the selection of a suitable plasticizer compatible with the film-forming polymer, and c) understanding the mechanism by which plasticizers improve the flexibility of coating films at the molecular and meso scales.

Various studies have been reported in the literature, investigating the effect of plasticizers on the properties of the final polymeric coating. Laboulfie et al. [1] studied the effect of plasticizer on the mechanical resistance and thermal behavior of composite coating films. They found that addition of a plasticizer (polyethylene glycol (PEG)) enhanced the plastic behavior of the HPMC-based coating films and improved its mechanical properties. Jarray et al. [2] also studied the affinity between polymers and coating additives in dry and aqueous systems. Saettone et al. [3] found that the drug release is influenced by the type and amount of the plasticizer.

In this work, we propose and compare four multi-scale approaches allowing to choose the adequate plasticizer and to formulate the right aqueous polymeric coating; the first approach is based on the generation of σ-profiles of the materials. σ-profiles present a map of the charge density over the surface of the molecule and provide information about the molecule and an understanding of the mutual solubilities of solvents [4]. The second approach is a molecular scale approach, based on the solubility parameter δ (i.e. the square root of the cohesive energy density). This parameter describes the intramolecular and intermolecular forces of a substance. It is a measure of the tendency of a molecule to interact with the surrounding molecules. The solubility parameter is used in the coating industry for selecting compatible solvents for coatings materials, and in surface characterization of fillers (e.g. calculation of interfacial energy associated

* Corresponding author at: Université de Toulouse, INP, UPS, LGC (Laboratoire de Génie Chimique), 4 allée Emile Monso, F-31432 Toulouse Cedex 04, France.
E-mail addresses: ahmed.jarray@ensiacet.fr (A. Jarray), vincent.gerbaud@ensiacet.fr (V. Gerbaud), mehrdji.hemati@ensiacet.fr (M. Hemati).

http://dx.doi.org/10.1016/j.porgcoat.2016.08.008

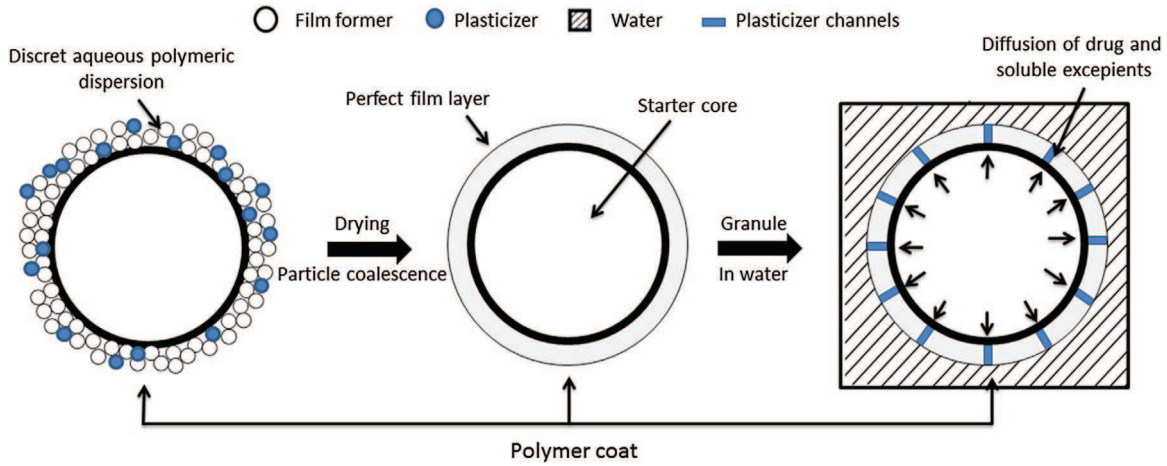

Fig. 1. Schematic representation of a typical film formation mechanism and plasticizer effect on drug release.

with stearic acid/water interface) [5]. The third approach is a mesoscale approach, where dissipative particle dynamics (DPD) simulation is used to investigate the structure of polymeric coating dispersion, where we follow the same DPD parameterization used by Jarray et al. [6]. The last approach is an experimental thermal analysis using differential scanning calorimetry (DSC). The developed approaches are tested for various systems composed of polyvinylpyrrolidone (PVP), microcrystalline cellulose (MCC), hydroxypropyl-methylcellulose (HPMC), polyethylene glycol (PEG) and water.

2. Film formers and plasticizer

2.1. Film formers

In general, film formers are organo-chemical macromolecule-forming substances that undergo a polymerization reaction and form crystalline or amorphous continuous structure as the coating dries. The role of the film former is to form a cohesive coating film on a given substrate and – where relevant – to hold together the components of the coating [7]. Film formation is the result of the increase in polymer concentration in the colloidal dispersion, leading to the formation of a three- dimensional network.

The formation of a polymeric film arises from the 'coalescence', i.e. deformation, cohesion and polymer chain interdiffusion, of the individual colloidal particles normally held apart by stabilizing forces [8]. Evaporation of the interstitial water upon drying leads to the deformation of the particles of polymer until complete coalescence (Fig. 1). This mechanism requires sufficient colloidal stability to form close packing upon coalescence; otherwise, poor film quality may be obtained. Film formation process also requires the spreading of the solution into a thin-layer. Keddie et al. [9] demonstrated that voids could remain in the film during film formation even after water evaporation.

The obtained film must be smooth and uniform. However, typically, film coating prepared from pure polymer tends to be brittle and crack upon drying. To overcome this problem, one way is to add a plasticizer to the coating dispersion.

2.2. Plasticizers in coating formulations

For polymers with limited film-formation ability, a plasticizer may be added to ease the deformation and to favor colloidal particles coalescence. The plasticizer partially eliminates the interactions responsible for the mechanical cohesion between the chains, and therefore increases their mobility. As a consequence, the rigid material is transformed into soft and flexible material [10]. Plasticizers reduce the glass transition temperature *Tg* and the minimum polymer film forming temperature (MFT) at levels that depend on the coating process. Plasticizers also create channels through which drug diffuses for pellets coated with insoluble films [11] (Fig. 1).

A good choice of a plasticizer depends on its compatibility with the polymer and on the permanence of the plasticizer in the film during coating. Compatibility between a polymer and a plasticizer produces stable and homogeneous coating film. It is often characterized by a high miscibility between the plasticizer and the polymer blend. Polymer-plasticizer incompatibility influences not only the mechanical properties but also drug release [12,13]. Permanence of a plasticizer means its tendency to remain in the plasticized material; i.e. long term compatibility. It depends on the size of the molecule and on its rate of diffusion.

Bodmeier and Paeratakul [14,15] studied the distribution of plasticizers between the aqueous phase and colloidal polymeric dispersions. They also studied the factors influencing the rate of diffusion of plasticizer through the polymer. During solid dosage forms coating preparation, for optimal mixing between the plasticizer and the polymeric dispersion, Bodmeier and Paeratakul recommended the introduction of water-insoluble plasticizer to the aqueous polymer dispersion before dilution of the latter. They also recommended a longer plasticization time for water-insoluble plasticizers than for water-soluble plasticizers. In his work on the coating of large Alumina particles, Ould-chikh [16] found that adding a plasticizer (Polyvinyl Alcohol (PVA)) in aqueous polymeric suspension reduces dramatically the segmentation or the cracking of the coating films upon drying.

3. Materials and methods

3.1. Materials

Our experimental study is elaborated with different materials widely used in food and pharmaceutical industries. The polymers are; PVP: polyvinylpyrrolidone (K10), MCC: microcrystalline cellulose (Avicel PH-101) and HPMC: hydroxypropyl-methylcellulose (E19). The chosen plasticizer is PEG400: polyethylene glycol 400. All the compounds are purchased from Sigma–Aldrich.

Polyvinylpyrrolidone or povidone (PVP) occurs as a fine, white to creamy-white colored, described as a synthetic polymer consisting essentially of linear 1-vinyl-2-pyrrolidinone groups [17]. Although PVP is used in a variety of pharmaceutical formulations, it is primarily used in solid-dosage forms. PVP solutions are used as binders in

Table 1
Composition of the different formulation studied throughout this paper.

Formulation name	Binder/coating composition (w/w)		
	Polymer	Plasticizer	Solvent
PEG 10%	–	10% PEG	90% water
HPMC-PEG 10%–10%	10% HPMC	10% PEG	80% water
PVP-PEG 10%–10%	10% PVP	10% PEG	80% water
MCC-PEG 10%–10%	10% MCC	10% PEG	80% water

HPMC: hydroxypropyl-methylcellulose, PVP: polyvinylpyrrolidone, MCC: microcrystalline.
cellulose, PEG: polyethylene glycol.

wet-granulation processes [18,19] and as a solubilizer in oral and parenteral formulations.

Microcrystalline cellulose (MCC) is purified cellulose, practically insoluble in water and in most organic solvents, produced by converting fibrous-cellulose to a redispersible gel or aggregate of crystalline cellulose using acid hydrolysis [20]. MCC is highly cohesive cellulose [21]. It is widely used in pharmaceuticals, primarily as a binder/diluent in oral tablet and capsule formulations where it is used in both wet-granulation and direct-compression processes [22].

Hydroxypropyl-methylcellulose or Hypromellose (HPMC) is a white or creamy-white fibrous or granular powder. It's available in several grades that vary in viscosity and extent of substitution [17]. It's soluble in cold water, forming a viscous colloidal solution; practically insoluble in hot water. Depending upon the viscosity grade, concentrations of 2–20% (w/w) are used for film-forming solutions to film-coat tablets. Lower viscosity grades are used in aqueous film-coating solutions. Compared with Methylcellulose, HPMC produces aqueous solutions of greater clarity, with fewer undissolved fibers present, and is therefore preferred in formulations for ophthalmic use [17].

Polyethylene glycols (PEG's) or macrogols are produced by polymerization of ethylene oxide in the presence of water. PEGs are widely used in a variety of pharmaceutical formulations and can be used to enhance the aqueous solubility or dissolution characteristics of poorly soluble compounds [23]. They are also useful as plasticizers in microencapsulated products to avoid rupture of the coating film when the microcapsules are compressed into tablets. When added to mixtures of HPMC, PEG improves the mechanical properties of the final coating product [1,24,25].

3.2. Preparation protocol of the samples

Polymer-plasticizer-water samples (PVP-PEG, HPMC-PEG and MCC-PEG in water) were prepared by adding the polymer in deionized water previously heated to 80 °C. The mixture was then homogenized by moderate agitation for 30–60 min using a rotor-stator homogenizer (Ultraturrax T25, Janke and Kunkel, Germany) at 85 °C. The plasticizer was then progressively added under agitation until it was evenly dispersed. The mixture was then cooled using an ice bath under agitation for 30 min. Solutions were thereafter degassed at 50 mbar for 2 h. To attain maximum stabilization, the readily prepared solutions were stored immediately at 5 °C for at least 24 h.

The samples were afterward spread on a glass plate using a CAMAG handcoater (Manufactured by CAMAG, Switzerland) to produce a thin film of 5 μm. The liquid films are then placed for 24 h at ambient temperatures. Table 1 presents the different formulations used throughout this study. Typically, the percentage of plasticizer in the coating dispersion is less than 10% (w/w). The reason we chose a high percentage of PEG equal to the percentage of the different polymers is double; i) To be able to see the mixing of PEG with the polymers in the DPD simulations, and ii) To clearly see the effect of adding PEG in the coating when using DSC analysis.

3.3. Methods

3.3.1. Method A: sigma profile

COSMO (Conductor-like Screening Model) [26] is a predictive model for the thermodynamic properties of fluids and solutions that combines quantum chemistry and statistical thermodynamics. In this model, the solvent is regarded as a homogeneous conducting medium but affected by a finite dielectric constant arising from a large number of electrostatic charges enveloping the surface of the solute molecule. The surface of this molecule bears a polarization charge density. To determine this density, quantum mechanics calculation based on the density functional theory (DFT) are launched in order to optimize the geometry of the molecule and to establish its electronic structure. Then, calculations based on the COSMO model are used to construct the charge density curve called sigma-profile. This profile is the probability $p(\sigma)$ of finding surface segment with the charge density σ [4]:

$$p(\sigma) = A_i(\sigma)/A_i \quad (1)$$

with $A_i(\sigma)$ the surface area with a charge density of value σ and Ai the total surface of the material i. COSMO employs molecular shaped cavities that represent the electrostatic potential by partial atomic charges. The results depend mainly on the van der Waals radii used to evaluate the cavity surface. The cavity surface is obtained as a superimposition of spheres centered at the atoms, discarding all parts lying on the interior part of the surface [26]. More details about COSMO can be found in Ref. [26].

Conductor-like Screening Model (COSMO) implemented in Dmol3 module as a part of Material Studio 7.0 package of Accelrys was used to generate the sigma-profiles of the molecules. Water is chosen as the solvent environment (relative dielectric constant = 78.54). A global orbital cutoff radius of 3.7 Å was used throughout the calculations. We have used the gradient-corrected functionals (GGA) of Perdew and Becke [27,28] for the geometry optimization and the COSMO calculations. It has been demonstrated by Perdew and Wang that this technique produces more reliable predictions than the Vosko-Wilk-Nusair (VWN) technique [29]. For best accuracy, we used the triple-numerical polarization (TNP) basis set [30]. In Dmol3-CSOMO [31], the radii of the spheres that make up the cavity surface are determined as the sum of the van der Waals radii of the atoms of the molecule and of the probe radius. First, geometry optimization was performed to bring the energy to obtain the most stable conformation and to adjust the coordinates of the atoms. The sigma profiles were thereafter generated. Complementary sigma profiles of a polymer and a plasticizer indicate good miscibility between them [4].

Fig. 2 shows the sigma profile of water as well as its COSMO surface. Water can act either as H-bond donor or H-bond acceptor. The σ-profile of water spans in the range of $\pm 0.02\,e\,Å^{-2}$. It is dominated by two major peaks arising from the strongly polar regions; the positive region (H-bond acceptor region) is due to the polar oxygen and the negative one (H-bond donor region) is due to the polar hydrogen atoms. The negatively charged surfaces of the water molecules appear blue and the positively charged ones appear red. Non-polar parts of the surface of the molecule are green. The peak arising from the positively polar hydrogens is located on the left side, at about $-0.015\,e\,Å^{-2}$. Most parts of the surface of water molecules are able to form more or less strong hydrogen bond. Hydrogen bonding is considered as weak up to $\pm 0.01\,e\,Å^{-2}$. Outside this limit, molecules can be regarded as strongly polar [4].

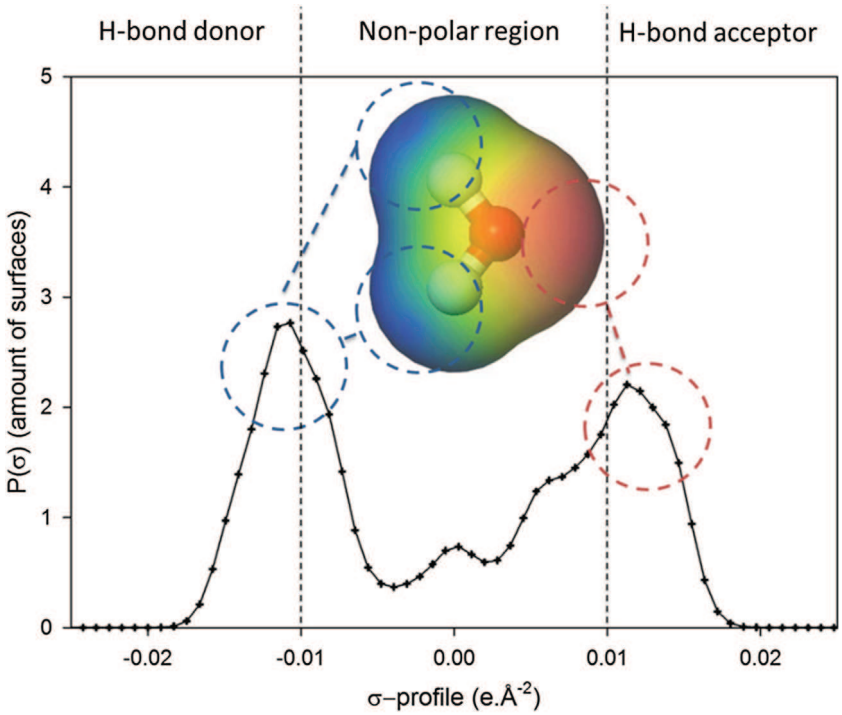

Fig. 2. σ-profile of water. (For interpretation of the references to colour in the text, the reader is referred to the web version of this article.)

3.3.2. Method B: solubility parameter via molecular simulations

3.3.2.1. Solubility parameter. The solubility parameter, δ (i.e. the square root of the cohesive energy density), describes the intramolecular and intermolecular forces of a substance. It is a measure of the tendency of a molecule to interact with the surrounding molecules. Solubility parameter has been proved useful for several pharmaceutical applications and has been correlated to a variety of properties [32] such as the surface tension, refractive index, work of adhesion and tensile strength. Solubility parameter was also used in the coating industry for selecting compatible solvents for coatings materials and also, in surface characterization of fillers [5].

In molecular simulation, the Hildebrand solubility parameter can be calculated from the pair potential by summing the pairwise interactions [33]. The cohesive energy density is equal to minus the intermolecular energy, i.e. the intramolecular energy minus the total energy:

$$\delta_k^2 = \frac{< \sum_{i=1}^{n} E_i^k - E_c^k >}{N_{av} < V_{cell} >} \quad (2)$$

with n the number of molecules in the simulation cell, N_{av} the Avogadro number, $k = 1, 2$, are the van der Waals energy (dispersion) and the coulombian energy (polar) respectively. ‹ ›denotes a time average over the duration of the dynamics in the canonical ensemble NVT, V_{cell} the cell volume, the index "i" refers to the intramolecular energy of the molecule i, and the index "c" represents the total energy of the cell.

As shown in the work of Hildebrand and Scott [34], the compatibility between a plasticizer and a polymer can be determined by the miscibility based on the solubility parameter. The enthalpy of the polymer (1) –plasticizer (2) mixture can be determined by:

$$\Delta H = v_{mix}\left(\left(\frac{\Delta E_2}{v_1}\right)^{1/2} - \left(\frac{\Delta E_1}{v_2}\right)^{1/2}\right)^2 x_1 x_2 - v_{mix}(\delta_1 - \delta_2) x_1 x_2 \quad (3)$$

where v_{mix} is the molar volume of the mixture, v_1 and v_2 are molar volumes of the polymer and the plasticizer respectively, ΔE_1 and ΔE_2 are molar energies of vaporization, x_1 and x_2 are volume fractions.

A plasticizer (1) and a polymer (2) are miscible in all proportion when $\delta_1 = \delta_2$ [35], which gives a positive value of the enthalpy of the mixture. This assumes that the Gibbs free energy of mixing ΔG is negative ($\Delta G = \Delta H - T\Delta S$) to allow solution formation. In this case, all the interactions between the molecules of the plasticizer and the polymer are of the same order of magnitude. The degree of miscibility between a plasticizer (1) and a polymer (2) increases as the square of the difference between the solubility parameters $\Delta\delta = (\delta_1 - \delta_2)^2$ decreases.

A similar approach was adopted by Price [36] to predict the compatibility between polymers and plasticizers, but he used group contribution method to calculate the solubility parameter, and found that the obtained values are underestimated. In this article, we will use molecular simulation to calculate the solubility parameter rather than group contribution methods. Jarray et al. [2] and Benali [37] used molecular simulations to calculate the solubility parameter and found good agreement with the experimental solubility parameter values.

3.3.2.2. Computation of the solubility parameter. For the computation of the solubility parameters, we run molecular simulations in the canonical ensemble NVT with the Forcite® module of the Material Studio Suite release 7 [31]. Simulations are run over 500 ps with a time step of 1 fs. The temperature is set at T = 298 K and controlled by a Nose Hoover thermostat with a Q ratio equal to 0.01. Energy and pressure stability was checked. The last 50 ps are used for averaging potential energy components. The average cohesive energy is computed to derive the solubility parameter by using equation (2). The standard deviation method can be evaluated by the block averages method [38]. Following the work of Jarray et al. [2], we estimated the average standard deviation as ten times the standard error given by Forcite [31].

COMPASSII (Condensed-phase Optimized Molecular Potentials for Atomistic Simulation Studies II) [39] forcefield was used with its predefined atom type parameters. Van der Waals interaction

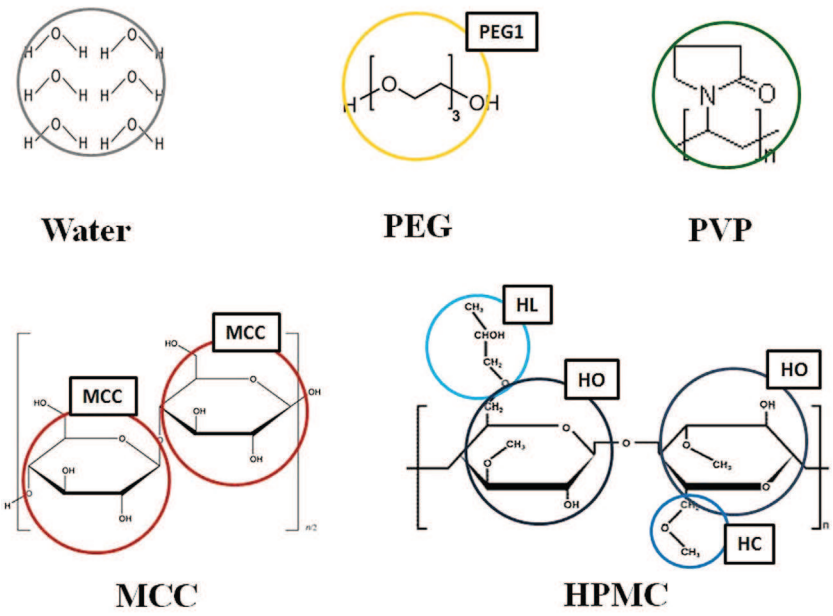

Fig. 3. "Coarse-grained" compounds; molecules and monomer conversion into equally sized beads.

was truncated by a spline function after 15.5 angströms. For the Coulombian interaction, partial charges were assigned by the predefined forcefield equilibration method, while the Ewald summation was used to account for the long-range interactions.

3.3.3. Method C: DPD method

3.3.3.1. Overview of the DPD method. The dissipative particle dynamics method (DPD) is a particle mesoscopic simulation method which can be used for the simulation of systems involving colloidal suspensions, emulsions, polymer solutions, Newtonian fluids and polymer melts. This method enables accessing larger spatiotemporal scales than those in the molecular dynamics.

Recently, a number of workers have used the DPD method for the simulation of polymer systems including Schulz et al. [40,41], Schlijper et al. [42], Tomasini and Tomassone [43], Jarray et al. [6] and Cao et al. [44]. Also, Gama Goicochea [45] used it to study polymer adsorption.

In the DPD method, the compounds are composed of molecules described as a set of soft beads that interact dynamically in a continuous space and move along the Newton momentum equation. These interactions between the soft beads govern the affinity between the compounds and therefore, control the final structure built by the beads in the DPD simulation.

An important parameter in the DPD method is the term $\bar{a}_{ij}$ of the conservative force, which represents the maximum repulsion between two unlike beads; it encompasses all the physical information of the system. It can be determined according to a linear relationship with the Flory-Huggins parameter χ_{ij}:

$$\bar{a}_{ij}(\bar{\rho} = 3) = \bar{a}_{ii} + \frac{\chi_{ij}}{0.286} \tag{4}$$

The number density $\bar{\rho}$ is equal to 3 DPD units, for which the repulsion parameter/Flory-Huggins parameter relationship has been defined [46]. The Flory-Huggins values can be calculated from the Hildebrand solubility parameter [34] using the formula:

$$\chi_{ij} = \frac{(\delta_i\text{-}\delta_j)^2(V_i + V_j)}{2k_BT} \tag{5}$$

with V the volume of the beads, δ_j and δ_i are the solubility parameters of beads i and j respectively.

For polymers, the number of beads that composes one polymer chain can be estimated with the number of DPD n_{DPD}:

$$n_{DPD} = \frac{M_w}{M_m C_n} \tag{6}$$

M_w is the molecular weight of the polymer, M_m the molecular weight of the monomer and C_n the characteristic ratio of the polymer. A detailed description of the DPD method is beyond the scope of this article but has been described in our previous work [6] and in the work of Groot and Warren [46].

3.3.3.2. DPD simulation parameters. In our DPD simulations, we used the same approach proposed by Jarray et al. [6]. Polymer and plasticizers molecules were coarse-grained into beads (see Fig. 3); A water bead represents 6 water molecules (volume of a water molecule ≈ 30 Å^3), which roughly corresponds to a single monomer of PVP, and to a half monomer of MCC. PEG400 is composed of three similar beads; each one contains the same fragment which we called PEG1. In the same way, HPMC repeating unit is coarse-grained into 4 beads (one HL, two HO and one HC) (Fig. 3).

The number of beads used to describe the HPMC polymer in the DPD simulations is determined by the DPD number n_{DPD} which was calculated using Eq. (6). The ratio characteristic was computed using Material Studio's [31] Synthia module [47]. We found that the HPMC polymer chain is composed of 10 repetitions ($n_{DPD} = 10$), and the MCC polymer is composed of 44 beads ($n_{DPD} = 44$). The conservative force parameters *aij* between every couple of beads is then calculated using the relationship (4). The results are summarized in Table 2.

All DPD simulations were performed within Materials Studio 7 software package [31]. A $30 \times 30 \times 30\, {r_c}^3$ (i.e. $24.4 \times 24.4 \times 24.4$ nm) simulation cell box was adopted where periodic boundary conditions were applied in all three directions. Initially, the beads were randomly dispersed in the simulation cell. Each DPD simulation ran for 1000 DPD units (i.e. 5374.17 ps) which was sufficient to get a steady phase. The integration time was taken as $t = 0.02$ DPD units (i.e. 107.48 fs). DPD simulations were run in the canonical thermodynamic NVT ensemble at a temperature of T = 298 K. The DPD parameters are summarized in Table 3.

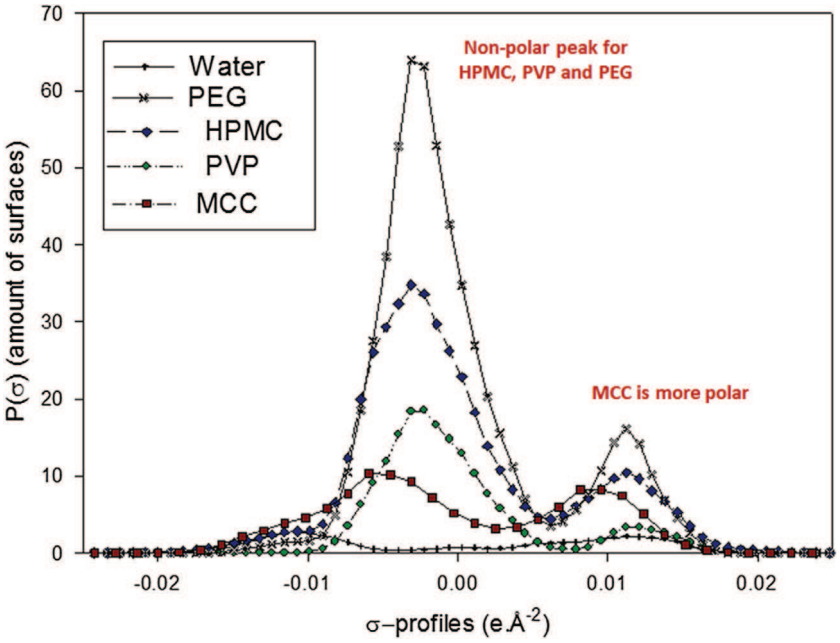

Fig. 4. σ-profile of water, PVP, HPMC, MCC and PEG400.

Table 2
The conservative force parameters $\bar{a}_{ij}$.

$\bar{a}_{ij}$		PVP	MCC	HL	HO	HC	PEG1	Water
PVP		157.00						
MCC		170.85	157.00					
HPMC	HL	157.00	170.5	157.00				
	HO	161.14	159.85	161.12	157.00			
	HC	159.09	179.56	158.82	167.56	157.00		
PEG1		157.38	167.64	157.43	159.26	161.33	157.00	
Water		256.78	198.64	252.37	222.05	260.48	253.79	157.00

PVP: polyvinylpyrrolidone, MCC: microcrystalline cellulose, HPMC: hydroxypropyl-methylcellulose, PEG: polyethylene glycol.

Table 3
List of parameters used in DPD simulations.

Number of molecules of water in one bead	6
Simulation box size	$24.4 \times 24.4 \times 24.4$ nm
Cut-off radius r_c	8.314 Å
Dissipation parameter γ	4.5 DPD units (i.e. 0.09043 g mol^{-1} fs^{-1})
DPD simulation time	1000 DPD units (i.e. 5374.17 ps)
Integration time	0.02 DPD units (i.e. 107.483 fs)
Temperature T	298 K

3.3.4. Method D: differential scanning calorimetry (DSC)

Differential scanning calorimetry (DSC) performs measurements of heat flow by varying the thermal energy supplied to the sample. This technique is particularly useful for determining the glass transition temperature *Tg* and the melting temperature *Tm*. Melting is a phase transition, characterized by the melting temperature *Tm*, that occurs when the polymer chains fall out of their crystal structures and become a disordered liquid.

In this work, the DSC tests were carried out with a differential scanning calorimetry analyzer DSC Q 2000. The software used for analysis of DSC data was Universal Analysis 2000 software analysis.

In the DSC instrument, the samples were sealed in DSC aluminum pan and scanned between 25–300 °C with a heating rate of 20 °C mn^{-1}. An empty aluminum pan served as reference. Each pan is in contact with a thermocouple connected to a computer. The registration of a signal proportional to the difference in the heat flow between these two pans is used to determine the melting temperature *Tm* and the melting enthalpy ΔH. The peak temperature of the melting endotherm in the DSC curves was taken to be the melting temperature *Tm* of the polymer. ΔH was calculated by integrating the melting peak's area for each sample.

In our DSC analysis, we studied more precisely the crystalline melting points of the films associated with the appearance of an endothermic peak in the DSC curves. This melting peak provides access to the melting temperature T_m, and to the energy required for melting different morphologies crystals.

To estimate the interaction between the materials in the blend, we used the Flory-Huggins theory [48]. The Flory-Huggins theory has provided a good empirical description of the mixing behavior of polymer-diluent systems and polymer–polymer systems [49,50]. Cao et al. [51] and Marsac et al. [52,53] used the Flory-Huggins theory for the estimation of polymer-solvent interaction using the melting point depression data obtained from DSC thermograms. Melting point depression is the reduction of the melting point of a polymer when mixed with another material and occurs when the two components are miscible or partially miscible [53]. Also, Nishi and Wang [54] used the Flory-Huggins theory for drug–polymer interaction. For the estimation of the Flory-Huggins interaction parameter χ between the plasticizer and a polymer, we have decided to use the same concept and we calculated χ using the following equation:

$$\frac{1}{T_m} - \frac{1}{T_m^0} = -\frac{R}{\Delta Hm}\left(\ln x_{plast} + \left(1 - \frac{1}{m_r}\right)\left(1 - x_{plast}\right) + \chi\left(1 - x_{plast}\right)^2\right) \quad (7)$$

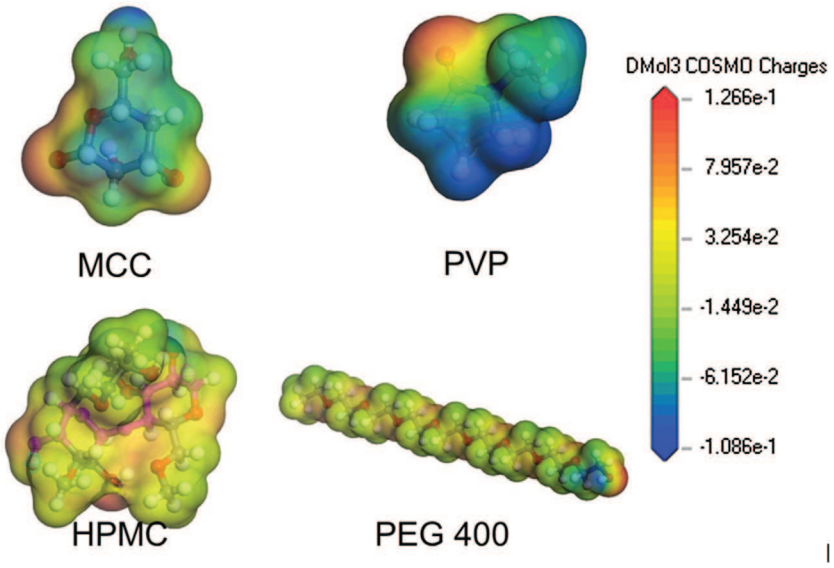

Fig. 5. Dmol3-COSMO surfaces of HPMC, PVP, MCC and PEG400.

where ΔHm is the melting heat of the pure plasticizer, T_m and $T^0{}_m$ are the melting temperatures of the plasticizer in the plasticizer-polymer mixtures and in the pure plasticizer respectively, R is the gas constant, x_{plast} is the volume fraction of the plasticizer and m_r is the ratio of the volume of the polymer repeating unit to that of the pure plasticizer.

A negative χ means that the attraction between a polymer–plasticizer pair is stronger than the average attraction between a polymer–polymer pair and a plasticizer–plasticizer pair (i.e., plasticizer–polymer attraction >½ (plasticizer–plasticizer + polymer–polymer) attraction). In this case, plasticizer molecules prefer to be in contact with polymer segments than with the plasticizer molecules. The more negative the value of χ, the stronger the attraction between the plasticizer and the polymer, the higher the miscibility, and vice versa; a positive value of χ indicates that the polymer and plasticizer molecules tend to be in contact with their own kind, leading to repulsion between the plasticizer and the polymer [55,56].

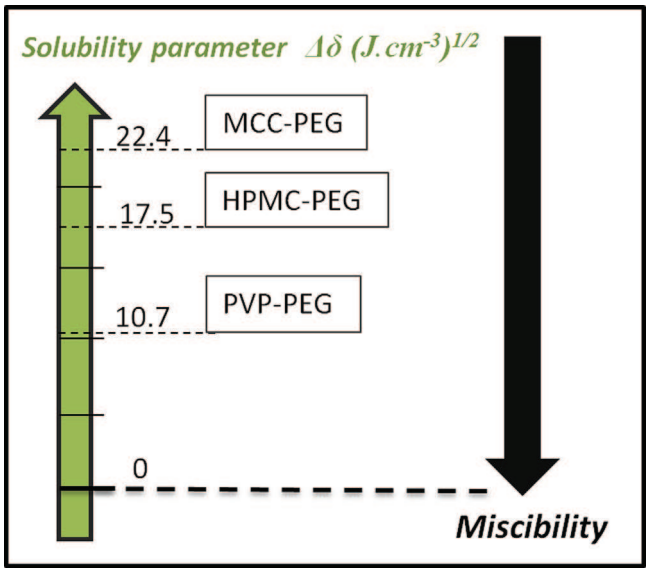

Fig. 6. Miscibility of HPMC, PVP and MCC with PEG400 predicted from the solubility parameter calculations.

Table 4
Solubility parameters calculated by molecular dynamics and experiments.

	Solubility parameter δ (J cm^{-3})$^{1/2}$	
	Molecular dynamics	Exp.
PVP	21.12 ± 0.16	–
MCC	29.98 ± 0.24	29.3 [57]
HPMC	20.68 ± 0.13	22.8 [58]
PEG400	22.88 ± 0.24	–
Water	47.78 ± 0.59	47.9 [32]

PVP: polyvinylpyrrolidone, MCC: microcrystalline cellulose
.HPMC: hydroxypropyl-methylcellulose, PEG: polyethylene glycol 400.

4. Results and discussions

4.1. Method A: σ-profiles

Fig. 4 shows the σ-profile of PVP, HPMC and PEG400, and compares them to that of a water molecule. Fig. 5 shows the COSMO surface of MCC, PVP, HPMC and PEG400.

HPMC has an asymmetric profile. An asymmetric profile means that the material does not feel comfortable in its pure state [4], i.e. there is an amount of electrostatic misfit. HPMC has a dominant peak in the non-polar region at −0.0029 e Å^{-2} and a small peak around 0.011 e Å^{-2} arising in the positive polar region, and another smaller shoulder extending from −0.01 to about 0.015 e Å^{-2} corresponding to the positively charged atoms. This suggests that HPMC molecules prefer to be in contact with a solvent showing hydrogen bond donor characteristic such as water.

PVP σ-profile, shown in Fig. 4, is also asymmetric, it has a major non-polar peak at −0.0028 e Å^{-2} and a smaller peak in the positive region of σ-profile, meaning that PVP can only act as H-bond acceptor and is looking for a H-bond donor. The polar oxygen in PVP does not find a partner with a reasonably negative σ; hence, when mixing with water, this misfit can be adjusted, and the polar oxygen may pair up with the polar hydrogen of water. PEG has a very similar curve shape to HPMC, suggesting solubility in water. From Fig. 4, we also notice that HPMC, PVP and PEG have similar σ-profile, this indicates a similar behavior in water and, considering that they are all looking for a H-bond donor, may suggest that they are miscible with each other if we consider the old chemical aphorism “similia similibus solvuntur” or “like dissolves like”. MCC molecule is polar and has two pronounced peaks at −0.005 e Å^{-2} and 0.009 e Å^{-2}.

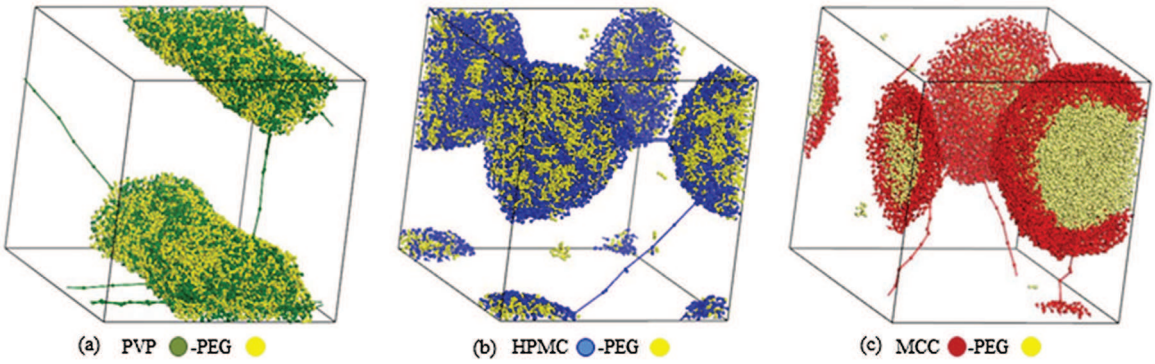

Fig. 7. Images of DPD simulation of PVP-PEG400, HPMC-PEG400 and MCC-PEG400 10%–10% (w/w) in water at the final simulation step.

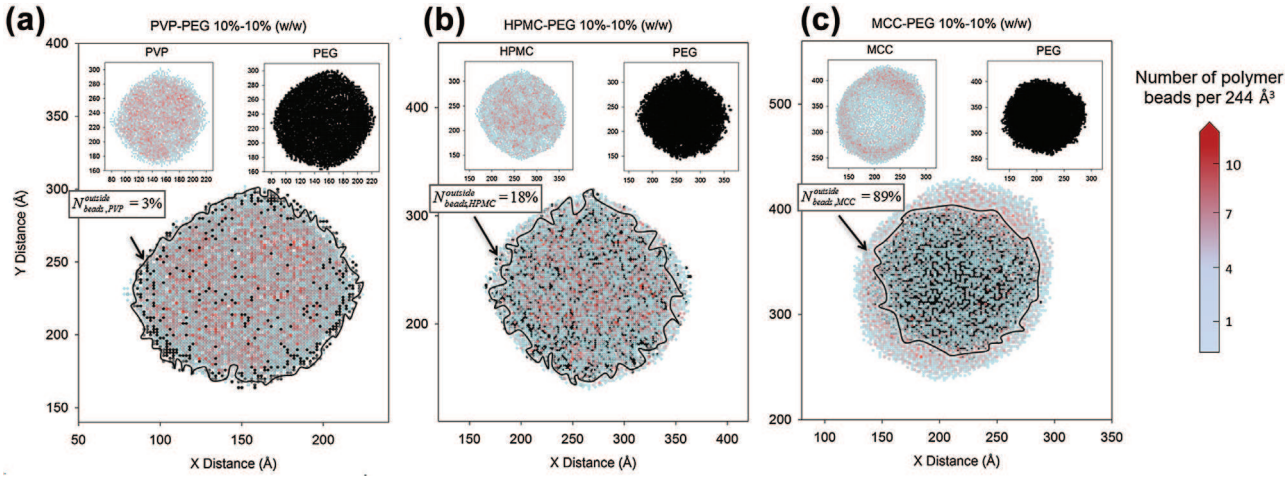

Fig. 8. Distribution of polymer beads (PVP, HPMC and MCC) around and through PEG.

In the negative σ-profile region, the position of the MCC peak is clearly shifted to the non-polar σ-profile range and both peaks are stronger than those exhibited by the water molecules. Both MCC and water have a similar symmetrical σ-profile, which means they feel comfortable in their pure state.

The conclusions obtained from COSMO are mostly interpretations based on charge distributions, and they do not provide a quantitative or a substantial qualitative method for assessing polymer-plasticizer compatibility. Nevertheless, the results can be compared to the remaining methods of this article.

4.2. Method B: solubility parameter δ

Table 4 compares experimental solubility parameters with those calculated by molecular simulations. We followed the same calculation method described above and proposed by Jarray et al. [2]. The average value of the cohesive energy density is obtained for all compounds from the last 50 picoseconds (ps) of the 500 ps dynamic simulation, spanning 500 000 time steps.

Table 4 shows that experimental Hildbrand solubility parameters values are close to the molecular simulation results. Jarray et al. [2] calculated the solubility parameter for different materials and also found that molecular simulation gives solubility parameter values close to the experimental ones.

Calculation of $\Delta\delta$ for PVP, MCC and HPMC with a plasticizer (PEG400) indicates the likelihood of miscibility between them (Fig. 6). PEG400 gives $\Delta\delta_{(PEG400\text{-}PVP)} = 10.7 < \Delta\delta_{(PEG400\text{-}HPMC)} = 17.5 < \Delta\delta_{(PEG400\text{-}MCC)} = 22.4\,J\,cm^{-3}$, showing that the miscibility decreases in the following order: PEG400-PVP > PEG400-HPMC > PEG400-MCC. This suggests that PVP and HPMC are more compatible with PEG400 as a plasticizer than MCC.

Method B based on the solubility parameter calculations can predict the compatibility between the film-forming polymer and the plasticizer; however, it does not provide information related to the structure of the blend, nor details regarding the interactions between the polymer chains and the plasticizer (i.e. diffusion of plasticizer in the polymer chains). In the next subsections, we will use DPD simulations to visualize the structure of the blend and we will compare the results to those obtained by method B.

4.3. Method C: DPD simulations

In this section, we examine the structure of PVP, HPMC and MCC in the presence of a plasticizer (PEG400) using DPD simulations. Polymer and plasticizer content in each mixture is fixed to 10% (w/w).

For a compound to be effective as a plasticizer, it must be able to diffuse into the polymer. The plasticizer will diffuse into the film-forming polymer with the rate and extent of diffusion being dependent on its water solubility and affinity for the polymer phase [35]. Plasticizers molecules act by inserting themselves between the polymer chains thereby extending and softening the polymer. This will improve the mechanical properties of the final film [35]. In Fig. 7(a) and (b), PVP and PEG as well as HPMC and PEG are well mixed, and PVP-PEG forms a tubular structure. In Fig. 7(c), MCC and PEG do not mix and MCC surrounds PEG beads.

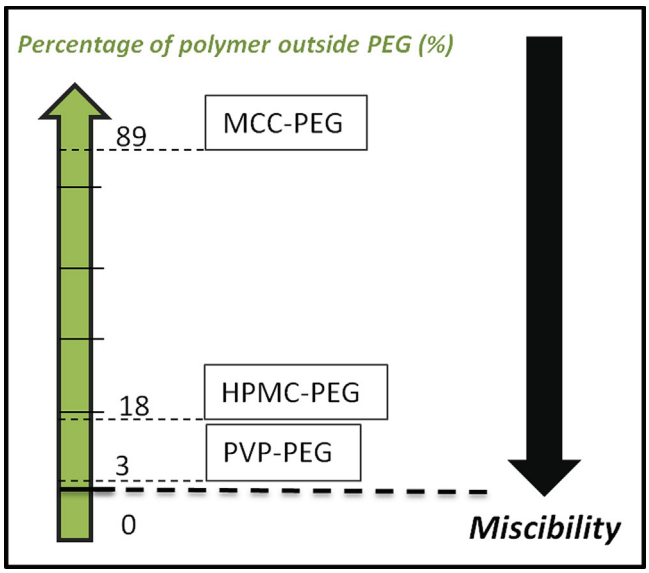

Fig. 9. Miscibility of HPMC, PVP and MCC with PEG400 predicted from the DPD simulations based on the percentage of polymer that does not mix with PEG400.

Fig. 8 shows the distribution of polymer beads (PVP, HPMC and MCC) around and through PEG plasticizer.

The percentage of beads of polymer that cover PEG network $N^{outside}_{beads,polymer}$ can be calculated by using the following equation:

$$N^{outside}_{beads,polymer} = \frac{100}{N_{Beads,polymer}}(N_{Beads,polymer} - \sum_i \Delta(\prod_j 1 \ \Delta(|r_o - r_i| + |r_i - r_j| - |r_o - r_j| \pm 2r_{water}))) \quad (8)$$

Where r_i denotes the position vector of the i^{th} polymer bead, $i = 1 \ldots N_{Beads,polymer}$. $N_{Beads,polymer}$ is the total number of polymer beads (HPMC, PVP or MCC in our case), r_j denotes the position vector of the j^{th} PEG bead, r_o is the position vector of the bead at the geometric center of the blend, r_{water} is the radius of a water bead which is roughly equal to the radius of the other beads, and Δ is the Dirac function.

Table 5
Melting temperature (Tm) and melting enthalpy (ΔHm).

	Tm (°C)	ΔHm (J g^{-1})
PEG	24.7	140.6
PEG in HPMC-PEG	6.3	32.5
PEG in MCC-PEG	16.8	38.1
PEG in PVP-PEG	9.61	37.2

In Fig. 8(a), PVP shows the highest percentage of beads inside PEG network (97% of PVP), meaning that PEG is a suitable plasticizer for PVP. PEG also mixes well with HPMC (Fig. 8(b)) with 82% of HPMC beads that diffuses through PEG and 18% of HPMC that surround PEG beads. MCC however, completely surrounds PEG with 89% of MCC beads outside PEG, forming a thicker external layer compared to the layers formed in all the other mixtures. This suggests that MCC is not compatible with PEG as a plasticizer. Fig. 9 summarizes the miscibility of the different blends based on the amount of PEG that does not mix with the polymer. PVP is more compatible with PEG than HPMC, and MCC shows the least compatibility. DPD conclusions are qualitatively similar to solubility parameter results (obtained using Method B).

4.4. Method D: DSC results

Fig. 10 shows photographs of the appearances of the samples used in this study and prepared using the protocol described in the previous section. PEG is soluble in water and forms a homogenous transparent solution (Fig. 10(a)). HPMC is also soluble in water and HPMC-PEG forms a transparent solution (Fig. 10(b)). MCC-PEG forms a white solution (Fig. 10(c)). PVP-PEG forms a transparent yellowish mixture (Fig. 10(d)). In all the mixtures, no phase separation can be observed by the naked eye.

DSC thermograms of the PEG400 and the films (HPMC-PEG, MCC-PEG, and PVP-PEG) were recorded using Differential Scanning Calorimeter and are presented in Fig. 11. The minimum of the DSC melting graph is the melting point that we denoted earlier by Tm. Table 5 presents the melting temperature (Tm) and melting enthalpy (ΔHm) obtained from the DSC analysis.

The thermal behavior of HPMC-PEG blend presents a low-temperature peak at 6.36 °C (enthalpy: 32.5 J g^{-1}). (Fig. 11). A decrease in the melting peak may indicate miscibility in

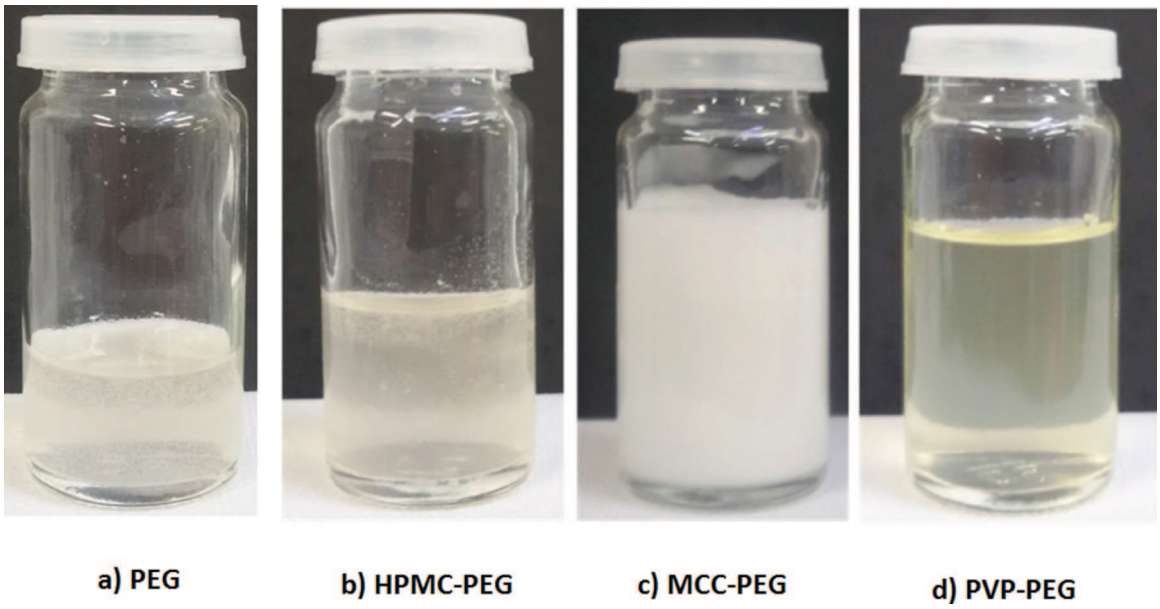

Fig. 10. Appearances of a) Pure PEG 10% (w/w), b) HPMC-PEG 10%–10% (w/w), c) MCC-PEG 10%–10% (w/w), d) PVP-PEG 10%–10% (w/w).

Table 6
Results summary table.

Mixture	DSC analysis	The different methods
HPMC-PEG	• HPMC forms more ordered crystal structure with fewer impurities than MCC • Partial miscibility between PEG and HPMC.	• PVP, HPMC and PEG have similar behavior in water (i.e. possible miscibility with each other) [A]. • HPMC and PVP are more compatible with PEG400 as a plasticizer than MCC [B] • Partial miscibility between PEG and HPMC [C].
PVP-PEG	• PEG is a good plasticizer for PVP (i.e. miscibility).	• High percentage of PVP diffuses in PEG network [C]. • PVP mixes with PEG in aqueous systems [B and C].
MCC-PEG	• MCC and PEG molecules show repulsion. • MCC is less compatible with PEG than PVP and HPMC.	• MCC surrounds PEG in aqueous systems [C]. • MCC is not compatible with PEG as a plasticizer [B and C].

A: COSMO, B: Solubility parameter and MD, C: DPD simulation.

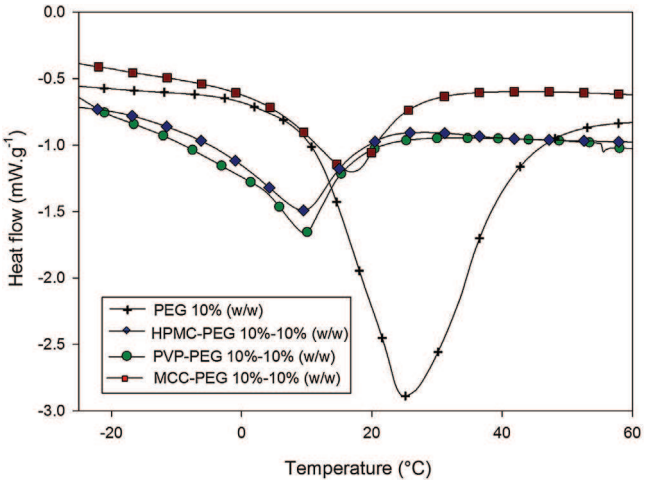

Fig. 11. DSC curves of PEG 10% (w/w), HPMC-PEG 10%–10% (w/w), MCC-PEG 10%–10% (w/w) and PVP-PEG 10%–10% (w/w).

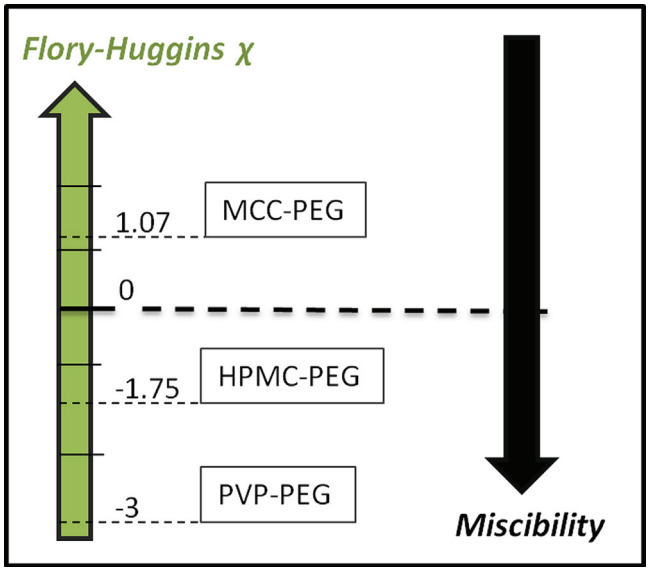

Fig. 12. Miscibility of HPMC, PVP and MCC with PEG400 predicted from the DSC results based on the Flory-huggins parameter.

drug–polymer system. Several research articles used this decrease of the melting temperature as an indicator of solid dosage forms polymer miscibility [59,60]. Mixing HPMC with PEG reduced the melting temperature of PEG from 24.7 to 6.3 °C (i.e. melting peak depression), indicating a substantial degree of mixing and miscibility. Adding PEG to HPMC enhances the chain mobility in the amorphous phase of HPMC, and HPMC-PEG blend crystallizes with more ease at lower temperatures.

MCC-PEG, on the other hand, presents an enthalpy event at 16.8 °C (enthalpy: 38.1 J g^{-1}). The melting peak temperature of PEG generated in the MCC-PEG blend is higher than the one generated in the HPMC-PEG blend, suggesting better interactions between HPMC and PEG than between MCC and PEG.

PVP-PEG DSC curve shows similar trends to the HPMC-PEG case with a slightly higher endothermic peak at 9.61 °C and melting enthalpy equal to 37.2 J g^{-1}, suggesting miscibility between PVP and PEG that is slightly lower than that of HPMC-PEG. However, as indicated by Meng et al. [56], the melting temperature decrease is not enough to claim that a plasticizer is compatible with a polymer. In the remaining of this section, we will use the Flory-Huggins theory to evaluate the polymer-plasticizer miscibility which is the same approach used by Cao et al. [51], Marsac et al. [52,53] and Nishi and Wang [54].

The melting temperature and the enthalpy extracted from the DSC thermograms are used for the calculation of the Flory-Huggins parameter χ. As emphasized in the previous section, a negative value of χ indicates that the polymer and the plasticizer are miscible in the melt, and the polymer–polymer interaction becomes stronger with the decrease of the value of χ [55,56]. Fig. 12 presents the Flory-Huggins interaction parameter of the different blends calculated using Eq. (7).

In the case of MCC-PEG, the positive value of $\chi = 1.07$ indicates repulsion between PEG and MCC molecules. This indicates immiscibility (Fig. 12) and therefore MCC is not compatible with PEG and may result in a less flexible film. Liew et al. [61] also found that MCC reduces the tensile strength and elasticity of the coating film containing PEG. The negative value of $\chi = -1.79$ in the HPMC-PEG blend indicates attraction between HPMC and PEG molecules. An attraction indicates miscibility and results in a flexible coating film. This is in adequacy with the experimental finding of Laboulfie et al. [1] who found that mixing PEG plasticizer with HPMC improves the mechanical properties of the coating film. Liew et al. [61] found that adding PEG to HPMC improves the elasticity of the resulting coating film. Regarding PVP-PEG blend, a larger negative value of $\chi = -3$ is obtained suggesting high attraction between PEG and PVP molecules, and consequently high miscibility. Barmpalexis et al. [62] found that PVP was completely miscible with PEG. In addi-

tion, Liew et al. [61] found that adding PVP to a composite coating film containing PEG increases both tensile strength and elasticity. Similarly, Dana et al. [63] also showed that the addition of PEG resulted in an increase in elasticity and adhesiveness of PVP-based hydrogels.

DSC results (Method D) are similar to DPD (Method C) and solubility parameter conclusions (Method B) obtained previously. DSC analysis showed partial miscibility of HPMC and PVP with PEG in the blend, but PVP interacts better with PEG than HPMC. In addition, there is repulsion between MCC and PEG indicating low compatibility. Similarly, from DPD simulations and solubility parameter calculation, we concluded that PVP is more compatible with PEG than HPMC and MCC.

5. Conclusion

In this study, different methods for the assessment of polymer-plasticizers compatibility were proposed and compared. We have used Dmol3 and COSMO model to generate σ-profiles of the compounds. We have seen that σ-profiles give valuable information regarding polarities, hb-donors and hb-acceptors, wich allow to guess the solubility of compounds. MCC has a different σ-profile shape than the other polymer (HPMC, PVP and PEG) and the curve suggests a low solubility in water. But the σ-profile results were not sufficient to predict the compatibility between PEG and the different polymers. We used molecular simulation rather than group contribution method for the calculation of the solubility parameter, and we found good agreement with the experiments. Calculation of solubility parameter δ using molecular simulations showed that PVP and HPMC are more compatible with PEG400 as a plasticizer than MCC.

DPD simulations showed that PEG plasticizer mix well with PVP indicating good compatibility between them. Partial diffusion of PEG through HPMC is obtained showing that there is partial miscibility between HPMC and PEG. However, PEG and MCC are not miscible, and MCC tends to cover PEG in water with a spherical shell. The experimental results obtained by DSC are similar to the DPD simulation results. It showed that there is a better interaction between HPMC and PEG than between MCC and PEG, and that HPMC shows a higher degree of miscibility and more attraction to PEG molecules than MCC. In addition, PEG is a good plasticizer for PVP.

Each method has its own advantage compared to the other methods; For example, the DPD method gives insights on the structure of the blends and predicts the amount of polymer diffused inside the plasticizer. COSMO method is faster but does not predict the extent of the compatibility. The DSC method is time-consuming and more expensive than the other methods.

Table 6 summarizes the results obtained by the different simulation methods and compares them with the results obtained by DSC.

References

[1] F. Laboulfie, M. Hemati, A. Lamure, S. Diguet, Effect of the plasticizer on permeability, mechanical resistance and thermal behaviour of composite coating films, Powder Technol. 238 (2013) 14–19.
[2] A. Jarray, V. Gerbaud, M. Hemati, Prediction of solid – binder affinity in dry and aqueous systems: work of adhesion approach vs. ideal tensile strength approach, Powder. Technol. 271 (2015) 61–75.
[3] M.F. Saettone, G. Perini, P. Rijli, L. Rodriguez, M. Cini, Effect of different polymer-plasticizer combinations on 'in vitro' release of theophylline from coated pellets, Int. J. Pharm. 126 (1995) 83–88.
[4] A. Klamt, COSMO-RS: From Quantum Chemistry to Fluid Phase Thermodynamics and Drug Design, Elsevier Science Ltd., Amsterdam, The Netherlands, 2005.
[5] C.M. Hansen, Hansen Solubility Parameters: A User's Handbook, Second edition, CRC Press, New York, 2007.
[6] A. Jarray, V. Gerbaud, M. Hemati, Structure of aqueous colloidal formulations used in coating and agglomeration processes: mesoscale model and experiments, Powder. Technol. 291 (2016) 244–261.
[7] T. Brock, M. Groteklaes, P. Mischke, European Coatings Handbook, 2nd revised edition, Hannover, Germany, 2010.
[8] P.A. Steward, J. Hearn, M.C. Wilkinson, An overview of polymer latex film formation and properties, Adv. Colloid Interface Sci. 86 (2000) 195–267.
[9] J.L. Keddie, P. Meredith, R.A.L. Jones, A.M. Donald, Kinetics of film formation in acrylic latexes studied with multiple-angle-of-incidence ellipsometry and environmental SEM, Macromolecules 28 (8) (1995) 2673–2682.
[10] G. Cole, J. Hogan, M.E. Aulton, Pharmaceutical Coating Technology, Informa Health Care, London, U.K, 1995.
[11] A.G. Ozturk, S.S. Ozturk, B.O. Palsson, T.A. Wheatley, J.B. Dressman, Mechanism of release from pellets coated with an ethylcellulose-based film, J. Control. Release 14 (1990) 203–213.
[12] K. Amighi, A. Moes, Influence of plasticizer concentration and storage conditions on the drug release rate from Eudragit RS 30 D film-coated sustained-release theophylline pellets, Eur. J. Pharm. Biopharm. 42 (1) (1996) 29–35.
[13] H. Arwidsson, O. Hjelstuen, D. Ingason, C.Gr. Affner, Properties of ethyl cellulose films for extended release. Part 2. Influence of plasticizer content and coalescence conditions when using aqueous dispersions, Acta Pharm. Nord. 3 (2) (1991) 65–70.
[14] R. Bodmeier, O. Paeratakul, The distribution of plasticizers between aqueous and polymer phases in aqueous colloidal polymer dispersions, Int. J. Pharm 103 (1) (1994) 47–54.
[15] R. Bodmeier, O. Paeratakul, Plasticizer uptake by aqueous colloidal polymer dispersions used for the coating of solid dosage forms, Int. J. Pharm. 152 (1) (1997) 17–26.
[16] S. Ould-Chikh, Elaboration, mise en forme et résistance mécanique de bi matériaux sphériques: application en catalyse, Thèse université de Lyon, Ecole Normale supérieure de Lyon, Lyon, France, 2008.
[17] R.C. Rowe, P.J. Sheskey, M.E. Quinn, Handbook of Pharmaceutical Excipients, 6th edition, Pharmaceutical Press, North Yorkshire, U.K, 2009.
[18] D. Becker, T. Rigassi, A. Bauer Brandi, Effectiveness of binders in wet granulation: comparison using model formulations of different tablet ability, Drug. Dev. Ind. Pharm. 23 (8) (1997) 791–808.
[19] L. Stubberud, H.G. Arwidsson, V. Hjortsber, C. Graffner, Water–solid interactions. Part 3. Effect of glass transition temperature, Tg and processing on tensile strength of compacts of lactose and lactose/polyvinyl pyrrolidone, Pharm. Dev. Technol. 1 (2) (1996) 195–204.
[20] J. Milani, G. Maleki, in: Benjamin Valdez (Ed.), Hydrocolloids in Food Industry in Food Industrial Processes – Methods and Equipment, 2012.
[21] M.T.M. Chitu, Granulation humide des poudres cohésives: rhéologie, mécanismes de croissance et tenue mécanique des granules, Thèse de Doctorat, Université de Toulouse, Toulouse, France, 2009.
[22] G.M. Enézian, La compression directe des comprimés à l'aide de la cellulose microcrystalline, Pharm. Acta. Helv. 47 (1972) 321–363.
[23] M.J. Miralles, J.W. McGinity, A. Martin, Combined water-soluble carriers for coprecipitates of tolbutamide, J. Pharm. Sci. 71 (1982) 302–304.
[24] J.T. Heinämäki, V.-M. Lehtolab, P. Nikupaavoa, J.K. Yliruusia, The mechanical and moisture permeability properties of aqueous-based hydroxypropyl methylcellulose coating systems plasticized with polyethylene glycol, Int. J. Pharm. 112 (1994) 191–196.
[25] J. Kundu, C. Patra, S.C. Kundu, Design, fabrication and characterization of silk fibroin-HPMC-PEG blended films as vehicle for transmucosal delivery, Mater. Sci. Eng. C 28 (2008) 1376–1380.
[26] A. Klamt, G. Schüürmann, COSMO: a new approach to dielectric screening in solvents with explicit expressions for the screening energy and its gradient, J. Chem. Soc. Perkin Trans. 2 (1993) 799–805.
[27] J.P. Perdew, Y. Wang, Accurate and simple analytic representation of the electron-gas correlation energy, Phys. Rev. B 45 (23) (1992) 13244–13249.
[28] A. Becke, D., A multicenter numerical integration scheme for polyatomic molecules, J. Chem. Phys. 88 (1988) 2547–2551.
[29] S.H. Vosko, L. Wilk, M. Nusair, Accurate spin-dependent electron liquid correlation energies for local spin density calculations: a critical analysis, Can. J. Phys. 58 (8) (1980) 1200–1211.
[30] B. Delley, Ground-state enthalpies: evaluation of electronic structure approaches with emphasis on the density functional method, J. Phys. Chem. A 110 (2006) 13632–13639.
[31] Biovia, Material Studio Suite Release 7, 2013 http://accelrys.com/products/materials-studio/index.html,.
[32] A.F.M. Barton, CRC Handbook of Solubility Parameters and Other Cohesion Parameters,U.S.A., 1991.
[33] M. Belmares, M. Blanco, W.A. Goddard 3rd, R.B. Ross, G. Caldwell, S.H. Chou, J. Pham, P.M. Olofson, C. Thomas, Hildebrand and Hansen solubility parameters from molecular dynamics with applications to electronic nose polymer sensors, J. Comput. Chem. 25 (2004) 1814–1826.
[34] J.H. Hildebrand, R.L. Scott, The Solubility of Nonelectrolytes, third edition, Reinhold Pub. Corp, New York, 1950.
[35] J.W. McGinity, L.A. Felton, Aqueous Polymeric Coatings for Pharmaceutical Dosage Forms, third ed., Marcel Dekker Inc., U.S.A, 2008.
[36] G.J. Price, Prediction of compatibility in polymer-plasticizer systems, Polymer 31 (9) (1990) 1745–1749.
[37] M. Benali, Prédiction des interactions substrat-liant lors de la granulation: Etude expérimentale dans un mélangeur à fort taux de cisaillement,

approches thermodynamiques par simulation moléculaire, thesis, INPT, Toulouse, France, 2006.
[38] H. Flyvbjerg, H.G. Petersen, Error estimates on averages of correlated data, J. Chem. Phys. 91 (1989) 461–467.
[39] H. Sun, COMPASS: an ab initio force-field optimized for condensed-phase applications overview with details on alkane and benzene compounds, J. Phys. Chem. B 102 (1998) 7338–7364.
[40] S.G. Schulz, U. Frieske, H. Kuhn, G. Schmid, F. Müller, C. Mund, J. Venzmer, The self-assembly of an amphiphilic block copolymer: a dissipative particle dynamics study, Tenside Surfact. Det. 42 (3) (2005) 180–183.
[41] S.G. Schulz, H. Kuhn, G. Schmid, C. Mund, J. Venzmer, Phase behavior of amphiphilic polymers: a dissipative particles dynamics study, Colloid Polym. Sci. 283 (3) (2004) 284–290.
[42] A.G. Schlijper, P.J. Hoogerbrugge, C.W. Manke, Computer simulations of dilute polymer solutions with the dissipative particle dynamics method, J. Rheol. 39 (3) (1995) 567–579.
[43] M.D. Tomasini, M. Tomassone, S., Dissipative particle dynamics simulation of poly(ethylene oxide)-pol(ethylethylene) block copolymer properties for enhancement of cell membrane rupture under stress, Chem. Eng. Sci. 71 (2012) 400–408.
[44] X. Cao, G. Xu, Y. Li, Z. Zhang, Aggregation of poly(ethylene oxide)-poly(propylene oxide) block copolymers in aqueous solution: DPD simulation study, J. Phys. Chem A. 109 (45) (2005) 10418–10423.
[45] A. Gama Goicochea, Adsorption and disjoining pressure isotherms of confined polymers using dissipative particle dynamics, Langmuir 23 (2007) 11656–11663.
[46] R.D. Groot, P.B. Warren, Dissipative particle dynamics: bridging the gap between atomistic and mesoscopic simulation, J. Chem. Phys. 107 (1997) 4423–4435.
[47] J. Bicerano, Prediction of Polymer Properties, CRC Press, New York, 2002.
[48] P.J. Flory, Theromdynamics of crystallization in high polymers. IV. A theory of crystalline states and fusion in polymers copolymers, and their mixtures with diluents, J. Chem. Phys. 17 (1949) 223–240.
[49] J. Martinez-Salazar, A. Alizadeh, J.J. Jimenez, J. Plans, On the melting behavior of polymer single crystals in a mixture with a compatible oligomer: 2. polyethylene/paraffin, Polymer 37 (1996) 2367–2371.
[50] J. Lyngaae-Jorgensen, Melting point of crystallites in dilute solutions of polymers. Poly(vinyl chloride) in tetrahydrofuran, J. Phys. Chem. 80 (1976) 824–828.
[51] J. Cao, F. Leroy, Depression of the melting temperature by moisture for alpha-form crystallites in human hair keratin, Biopolymers 77 (2005) 38–43.
[52] P.J. Marsac, S.L. Shamblin, L.S. Taylor, Theoretical and practical approaches for prediction of drug?polymer miscibility and solubility, Pharm. Res. 23 (2006) 2417–2426.
[53] P.J. Marsac, T.L. Li, L.S. Taylor, Estimation of drug–polymer miscibility and solubility in amorphous solid dispersions using experimentally determined interaction parameters, Pharm. Res. 26 (2009) 139–151.
[54] T. Nishi, T.T. Wang, Melting point depression and kinetic effects of cooling on crystallization in poly(vinylidene fluoride)-poly(methyl methacrylate), Macromolecules 8 (6) (1975) 909–915.
[55] N.R. Choudhury, P. De Prajna, Dutta K.N, Thermal Analysis of Rubbers and Rubbery Materials, Smithers Rapra Technology, U.K, 2010.
[56] F. Meng, V. Dave, H. Chauhan, Qualitative and quantitative methods to determine miscibility in amorphous drug?polymer systems, Eur. J. Pharm. Sci. 77 (2015) 106–111.
[57] R.C. Rowe, Interactions in coloured powders and tablet formulations: a theoretical approach based on solubility parameters, Int. J. Pharm. 53 (1989) 47–51.
[58] R.C. Rowe, Polar/non-polar interactions in the granulation of organic substrates with polymer binding agents, Int. J. Pharm. 56 (1989) 117–124.
[59] T.P. Lodge, E.R. Wood, J.C. Haley, Two calorimetric glass transitions do not necessarily indicate immiscibility: the case of PEO/PMMA, J. Polym. Sci. 44 (2005) 756–763.
[60] S.-Y. Chan, S.D.Q.M. Qia Craig, An investigation into the influence of drug–polymer interactions on the miscibility, processability and structure of polyvinylpyrrolidone-based hot melt extrusion formulations, Int. J. Pharm. 496 (2015) 95–106.
[61] K.B. Liew, Y. Tze Fung Tan, K.-K. Peh, Effect of polymer, plasticizer and filler on orally disintegrating film, Drug Dev. Ind. Pharm. 40 (1) (2014) 110–119.
[62] P. Barmpalexis, I. Koutsidis, E. Karavas, D. Louka, S.A. Papadimitriou, D.N. Bikiaris, Development of PVP/PEG mixtures as appropriate carriers for the preparation of drug solid dispersions by melt mixing technique and optimization of dissolution using artificial neural networks, Eur. J. Pharm. Biopharm. 3 (2013) 1219–1231 (Pt. B).
[63] S.F. Dana, D.-V. Nguyen, J.S. Kochhar, X.-Y. Liubcde, L. Kang, UV-curable pressure sensitive adhesive films: effects of biocompatible plasticizers on mechanical and adhesion properties, Soft Matter 9 (2013) 6270–6281.